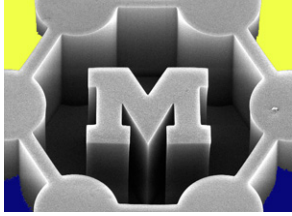

09: **Wetting and small-scale fluid flows**

February 10, 2010

John Hart
ajohnh@umich.edu
http://www.umich.edu/~ajohnh

Announcements

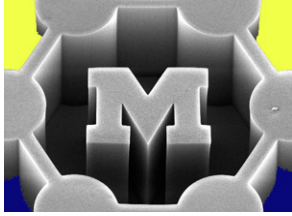

- Video assignment posted
  - Form a team and choose a topic
  - Q&A at beginning of lecture on Monday

Recap: surface energy and melting

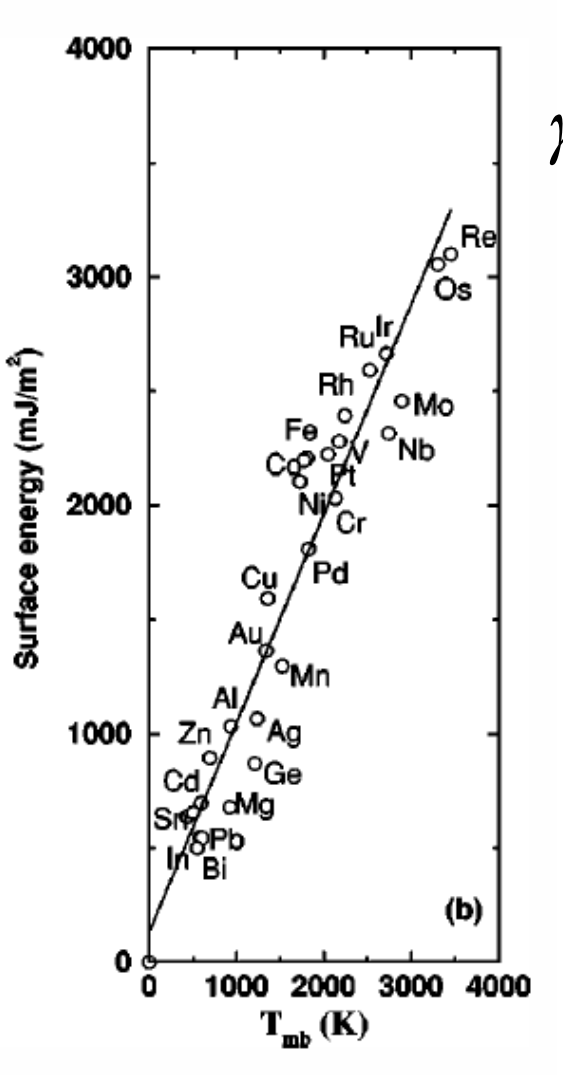

$$\gamma = \frac{A}{24\pi D_o^2}$$

$$T_{m,nano} = T_{m,bulk}\left(1 - \frac{2\gamma_{sl}}{h_o r}\right)$$

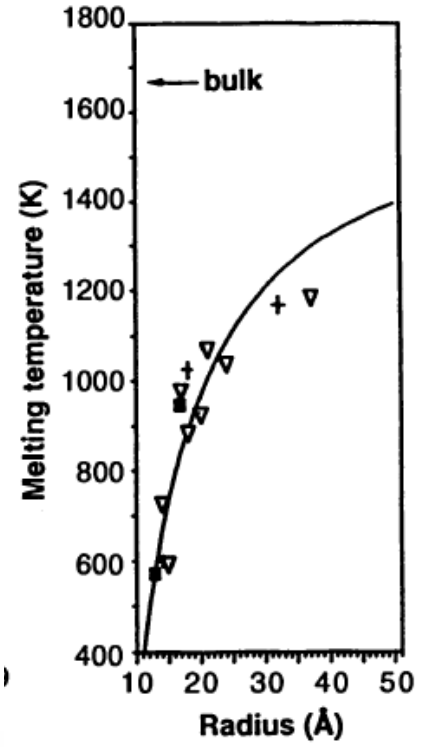

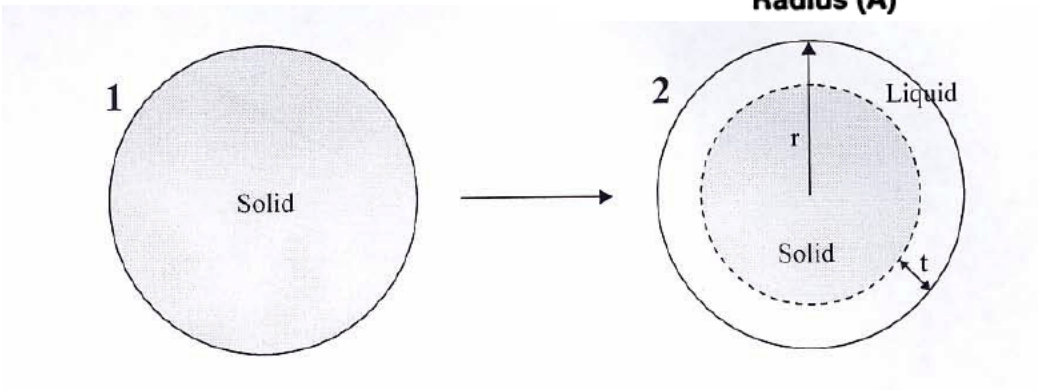

Nanda et al., Phys. Rev. B 66:013208, 2002.
Goldstein et al., Science 256:1425, 1992.

Today's agenda

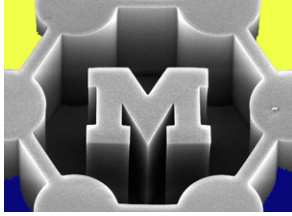

- Engineering surface texture to control wetting behavior
- Micro/nanoscale effects on fluid flows –analogy to classical (rarefaction) and quantum (surface) size effects
- Modeling slip flows in small pipes
- Measurements of slip flows

Today's readings

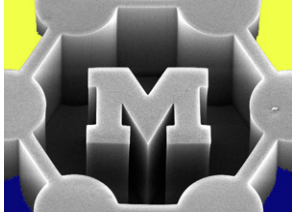

From last time:

- Tuteja et al., "Design parameters for superhydrophobicity and superoleophobicity"

Nominal: (ctools)

- Karniadakis, excerpt on breakdown of the continuum fluid hypothesis, from Micro Flows
- Arkilic et al., "Gaseous slip flow in long microchannels"
- Eijkel, "Liquid slip in micro- and nanofluidics: recent research and its possible implications"

Extras: (ctools)

- Majumdar et al., "Enhanced flow in carbon nanotubes"
- Holt et al., "Fast mass transport through sub-2-nanometer carbon nanotubes"

Wetting

- Wetting is the ability of a liquid to maintain contact with a solid surface, resulting from intermolecular interactions when the liquid and solid are brought together.
- Thus, wetting is determined a balance between adhesive and cohesive forces, which determine the overall free energy.

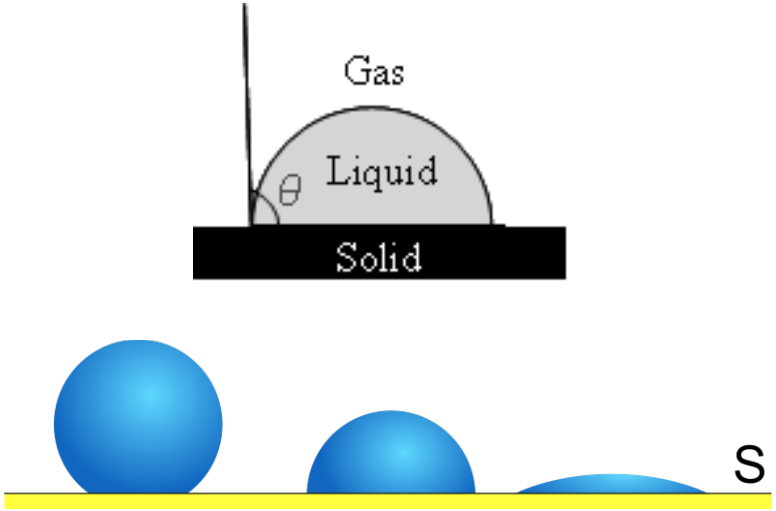

Contact angle	Degree of wetting	Strength of:	
		S/L interactions	L/L interactions
θ = 0	Perfect wetting	strong	weak
0 < θ < 90°	high wettability	strong	strong
		weak	weak
90° ≤ θ < 180°	low wettability	weak	strong
θ = 180°	perfectly non-wetting	weak	strong

- Liquids more frequently wet solids having high surface energy (i.e., strongly bonded solids) than solids with low surface energy (i.e., VDW solids). It's practically difficult to prevent low surface energy liquids from wetting solids.

Hydrophilic or hydrophobic? (see videos)

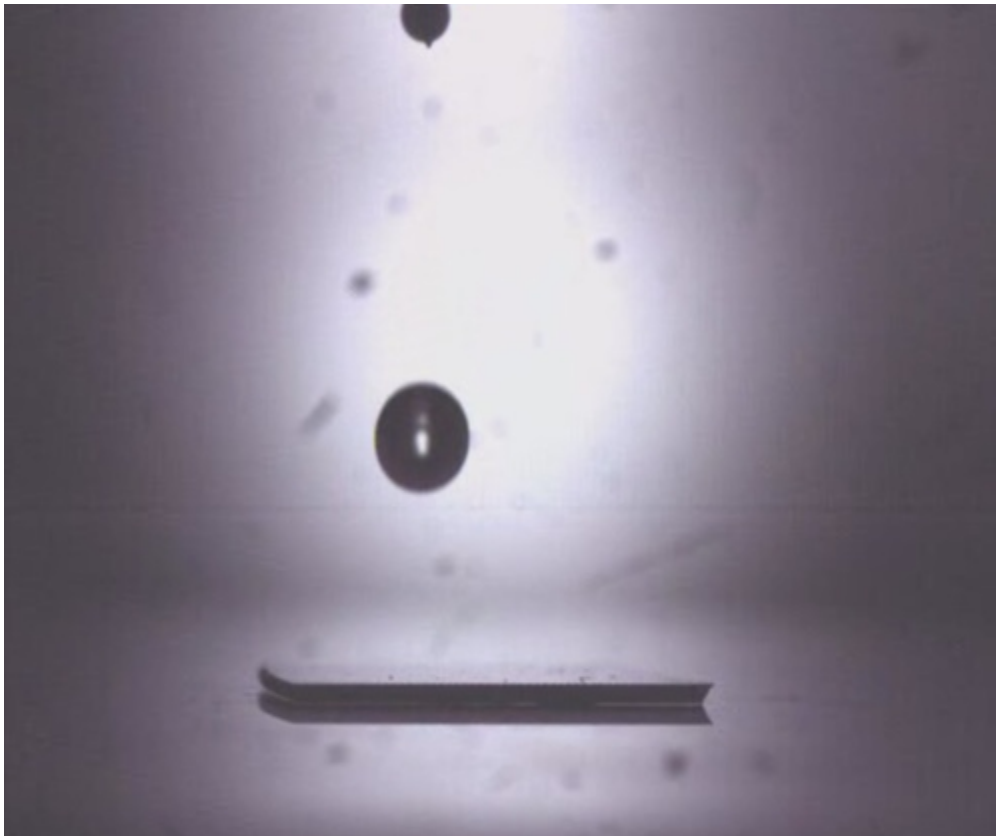

Courtesy of Hyungwoo Lee, MIT

Superhydrophobicity: petal and lotus effects

- Rose petals and lotus leaves are both superhydrophobic; however, droplets roll off lotus leaves but do not roll off rose petals

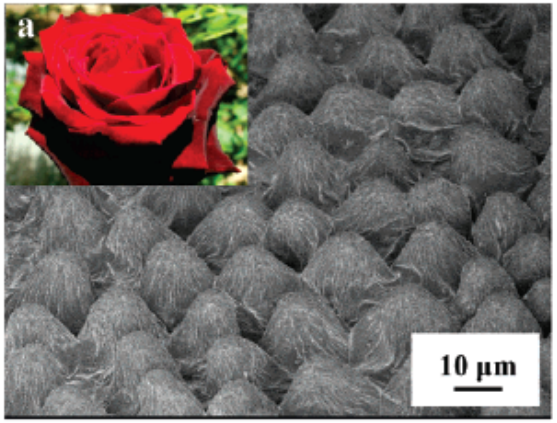

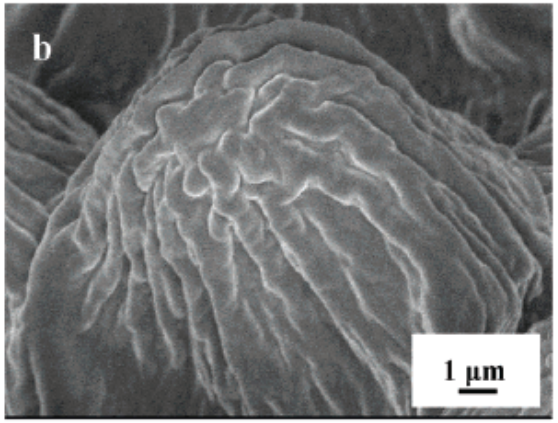

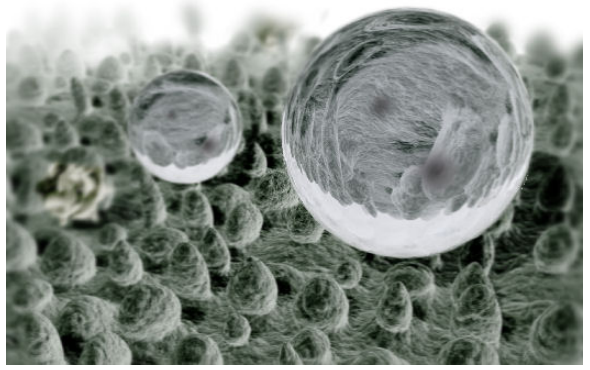

- We can engineer wetting by systematic control of surface energy and topography

Feng et al., Langmuir 24(8):4114-4119, 2008.

Textured surfaces: Cassie and Wenzel states

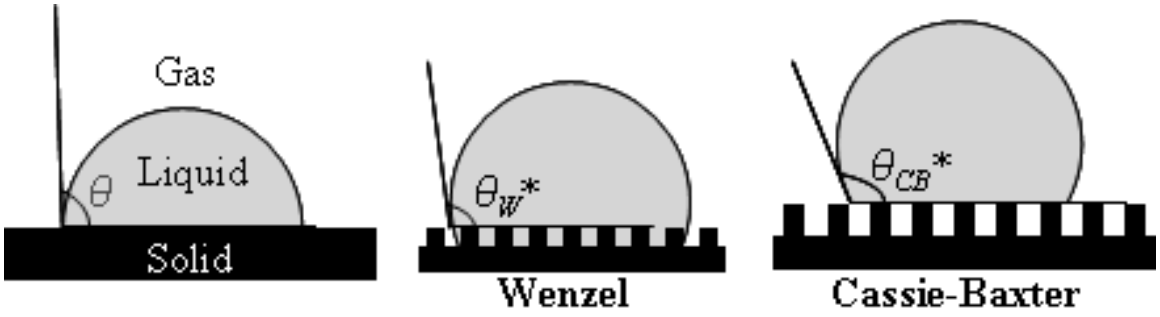

Advancing and receding contact angles –multiple stable contact angles

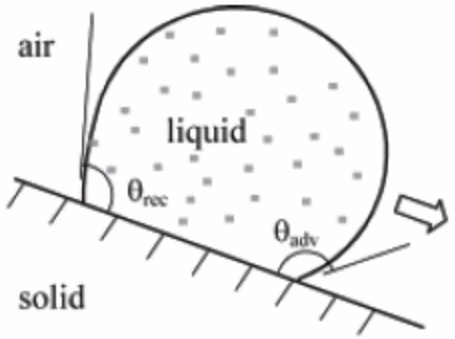

14-μm diameter, 30-μm height,and 105-μm pitch pillars

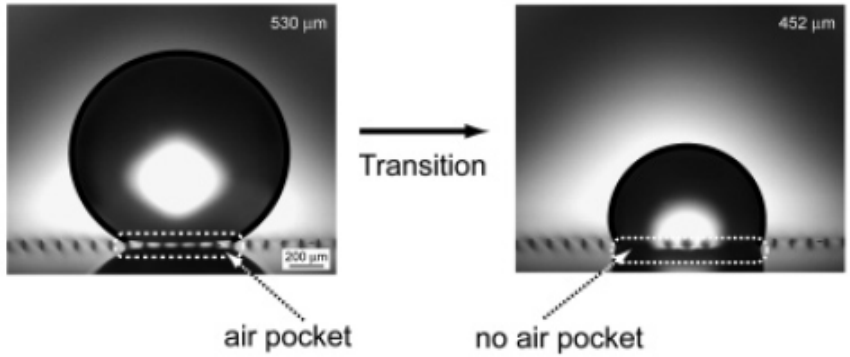

Droplet condensation and growth in ESEM

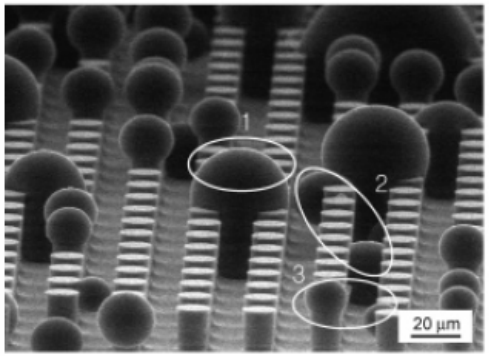

Water droplets in 1, 2, 3 appear

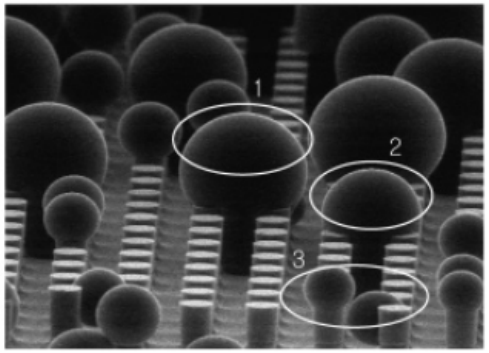

Water droplets in 2 merge

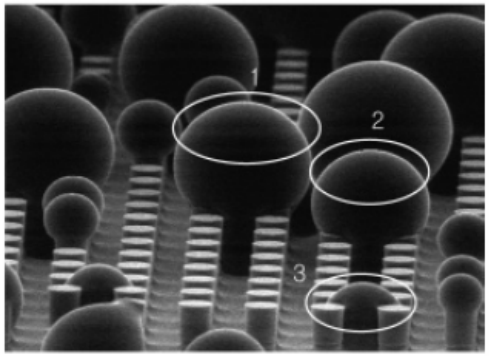

Water droplets in 3 merge

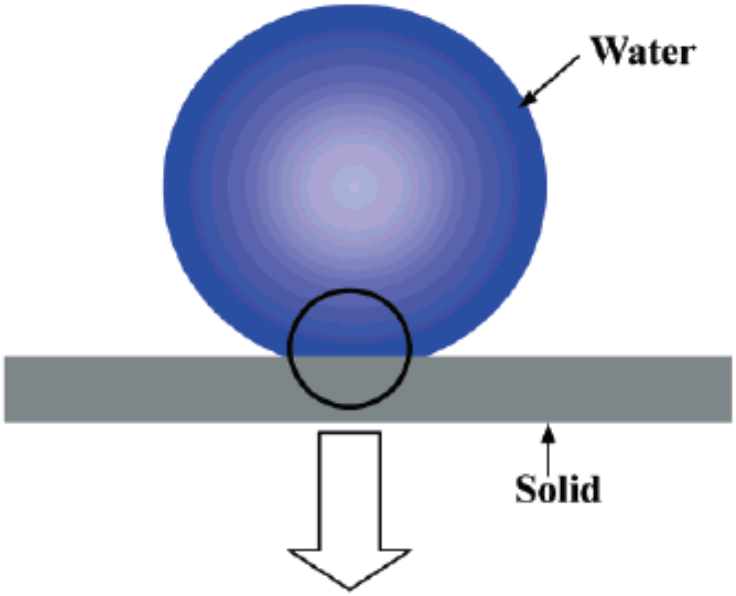

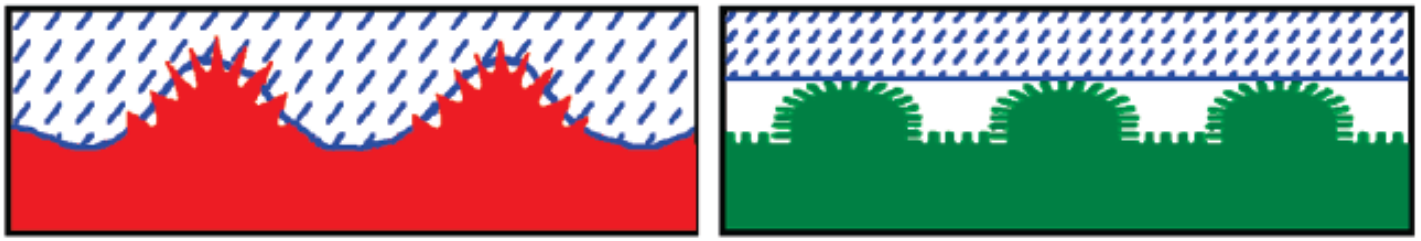

Petal (Cassie impregnating wetting state)

Lotus (Cassie's state)

Figure 3. Schematic illustrations of a drop of water in contact with the petal of a red rose (the Cassie impregnating wetting state) and a lotus leaf (the Cassie's state).

Feng et al., Langmuir 24(8):4114-4119, 2008.

Texture + chemistry: PTFE-coated CNT forest

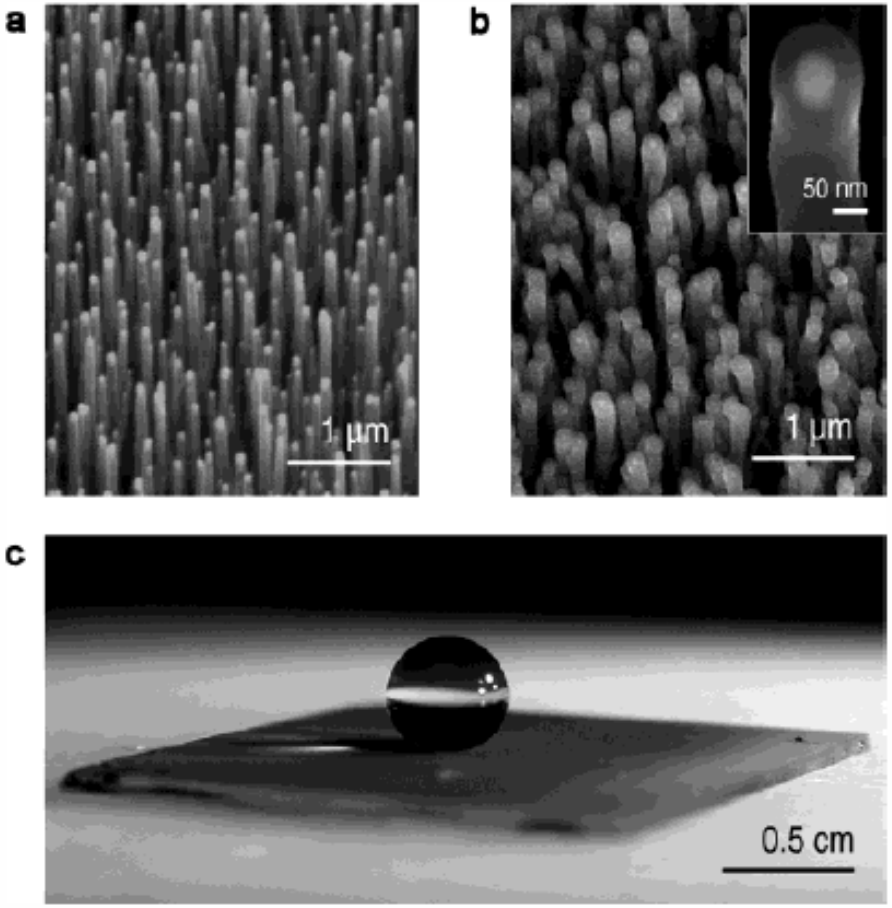

Figure 1. SEM images of carbon nanotube forests. (a) As-grown forest prepared by PECVD with nanotube diameter of 50 nm and a height of 2 μm, (b) PTFE-coated forest after HFCVD treatment, and (c) an essentially spherical water droplet suspended on the PTFE-coated forest.

Lau et al., Nano Letters 3(12):1701-1705, 2003.

Apparent contact angle of microstructures

- Stable composite interface

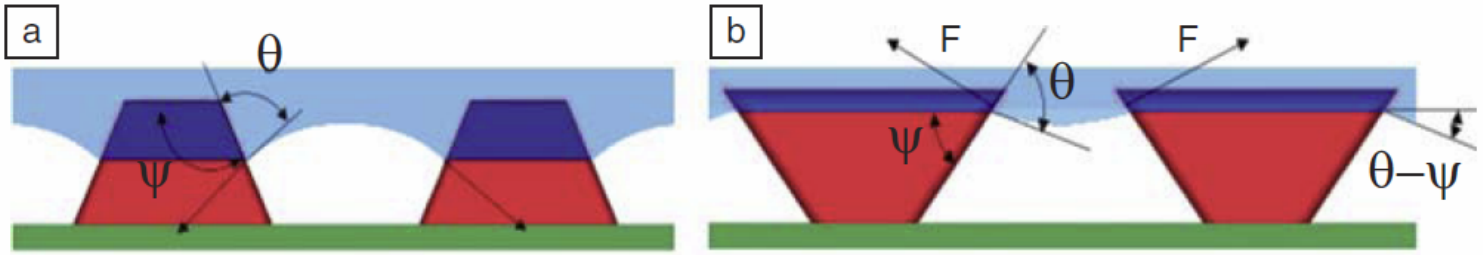

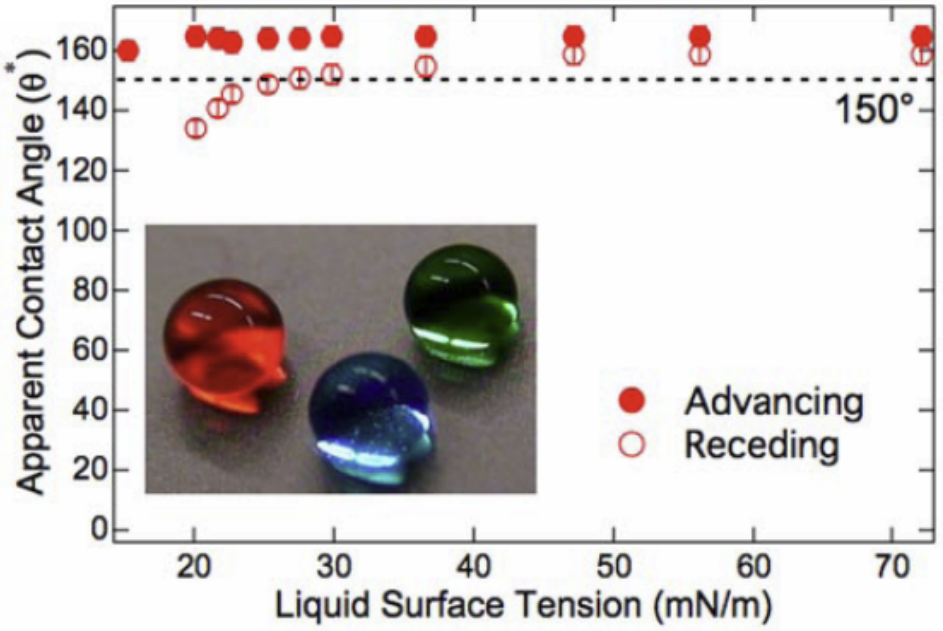

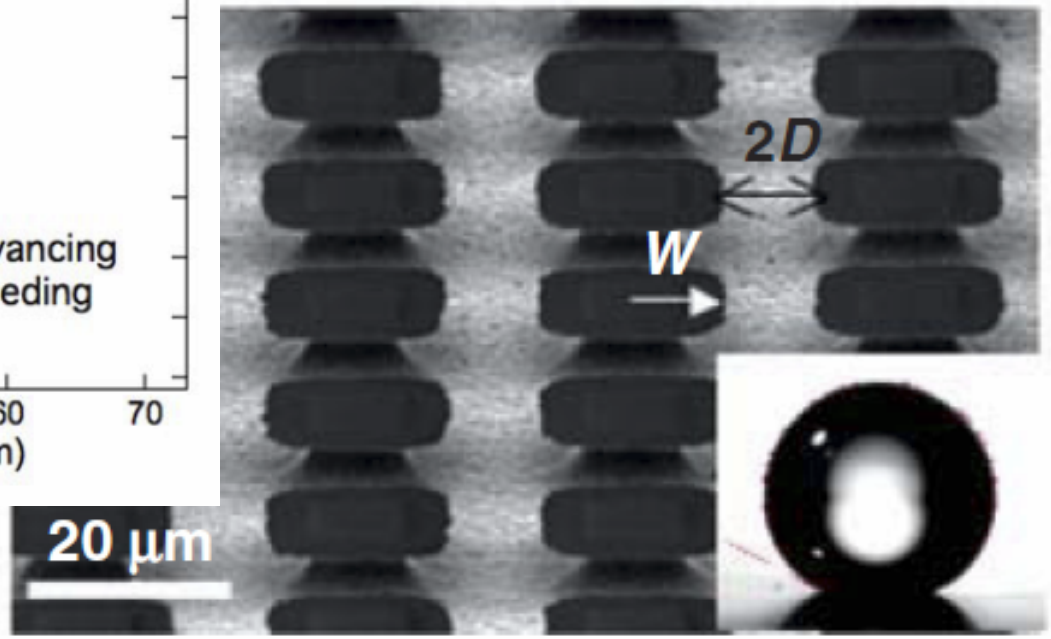

Tuteja et al., MRS Bulletin 33:752-758, 2008.
Tuteja et al., PNAS 105(47):18200-18205, 2008.

What's different about small-scale flows

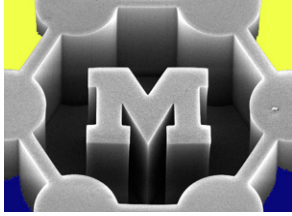

- As the length scale (e.g., pipe diameter) decreases, molecular interactions with the walls become more frequent. Friction also increases as surface-volume ratio increases.
- High pressure drops over short lengths mean compressibility of gases is important.
- Molecular interactions determine relative velocity (slip) at the wall, which reduces friction.
- Molecules can order (and crystallize) when confined.

- Flow regimes are classified based on the Knudsen number.

Classification of flow regimes

Knudsen number (Kn)

$$\mathrm{Kn} = \lambda / L_o$$

Gases, *l* = mean free path

$$\mathrm{Kn} = b / L_o$$

Liquids, *b* = slip length

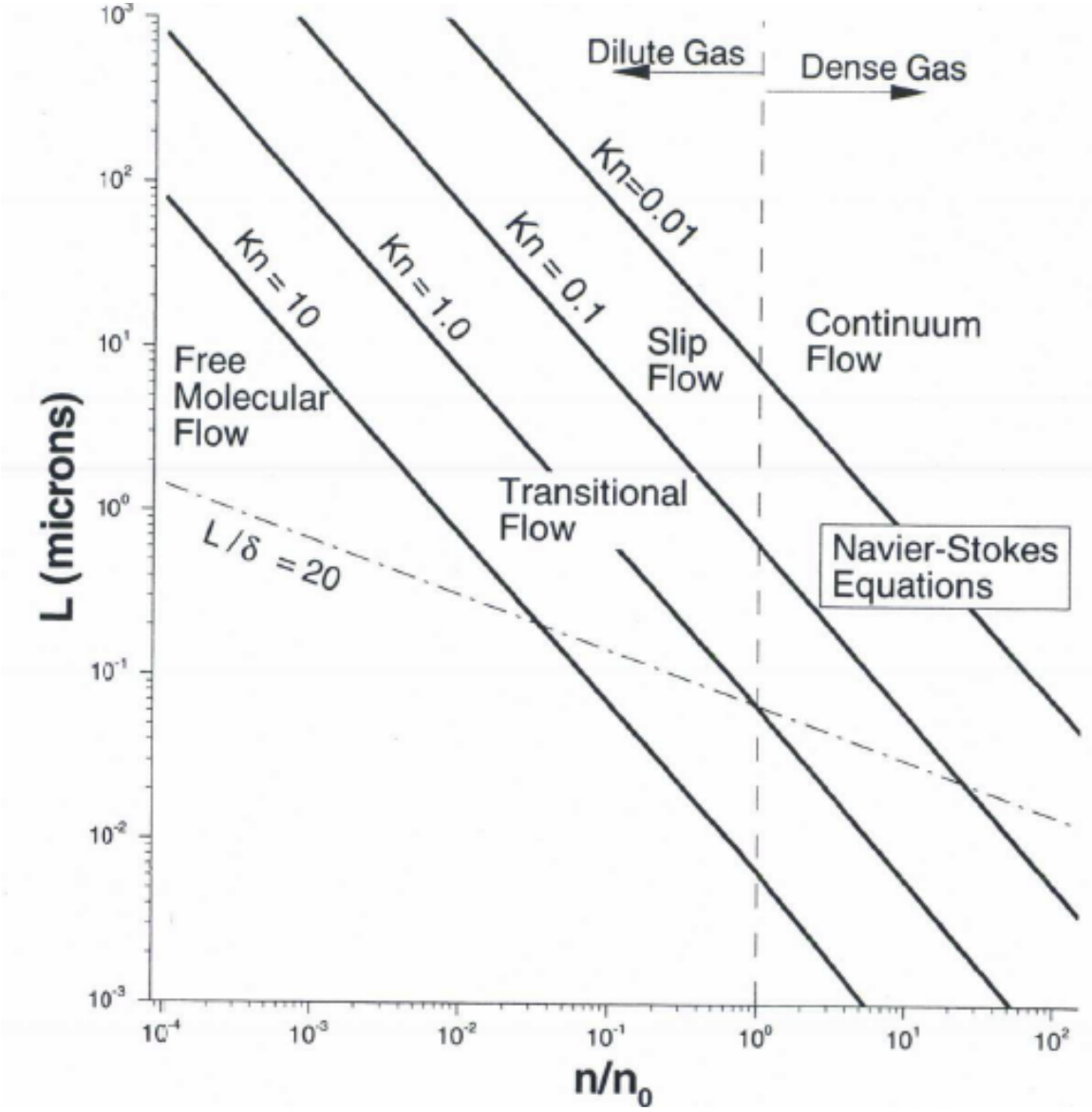

FIGURE 1.9. Limits of approximations in modeling gas micro flows. L (vertical axis) corresponds to the characteristic length and n/n_o is the number density normalized with corresponding atmospheric conditions. The lines that define the various Knudsen number regimes are based on air at *isothermal* conditions at $T = 273\,K$. Statistical fluctuations are significant below the line $L/\delta = 20$.

Karniadakis and Beskok.

Ideal gas

$$Kn = \lambda / L_0 = \lambda / D$$

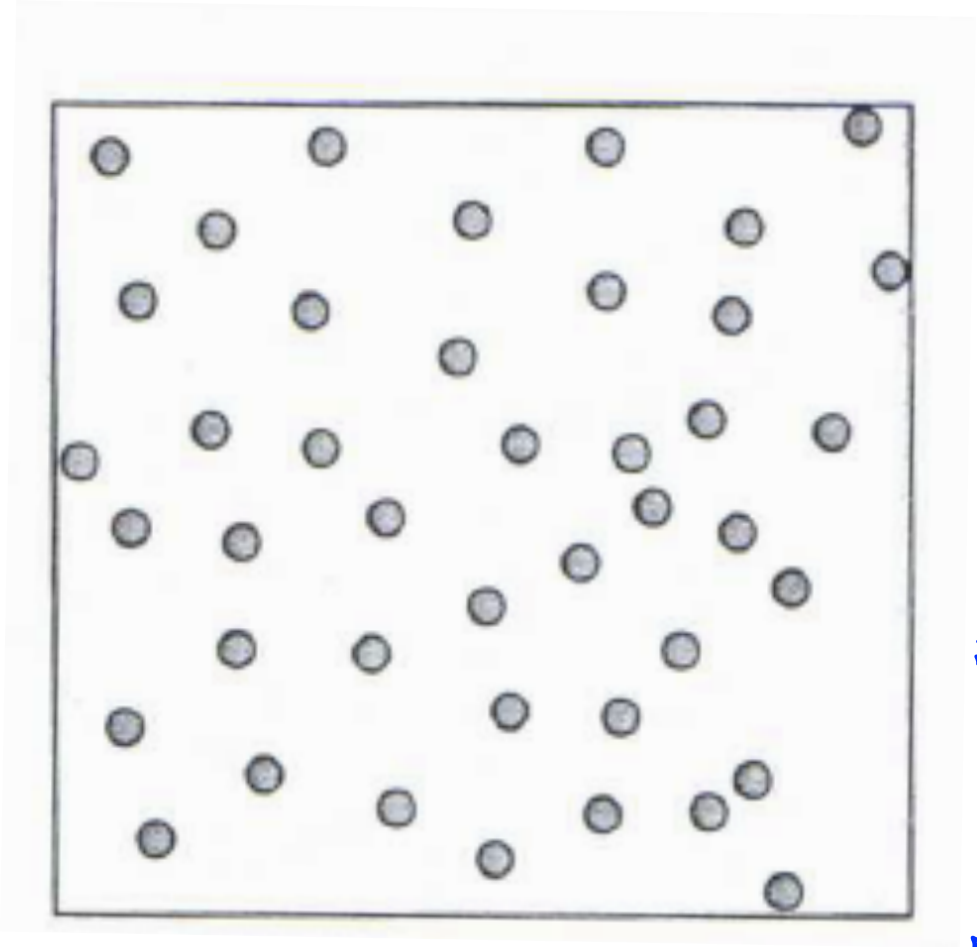

dilute gases $\delta / d >> 1$

ideal gas law

$$p = n k_B T$$

k_B: 1.38 E-23 J/K

n: 2.7 E25 Molecules/m^3

mean molecular spacing

$$\delta \approx n^{-1/3} \approx 3 \text{ E-9 M}$$

3 nM

Molecular diameter

$$d \approx 10^{-10} \text{ M} \approx 1 \text{ Å}$$

$$\lambda = \frac{1}{\pi d^2 n \sqrt{2}} = \frac{k_B T}{\pi p d^2 \sqrt{2}}$$

d: hard-sphere diameter

n: # density f(pressure)

$Kn < 0.01$ continuum (no slip)

$0.01 < Kn < 0.1$ slip

$0.1 < Kn < 10$ "transition"

λ examples: air

air @ 1 atm, 300 K, $\lambda = 65$ nm $\Big\}$ $Kn < 0.01$

@ 0.001 atm, 300K $\lambda = 65$ μm! $D > 6500$ μm λ/D

6.5 mm!

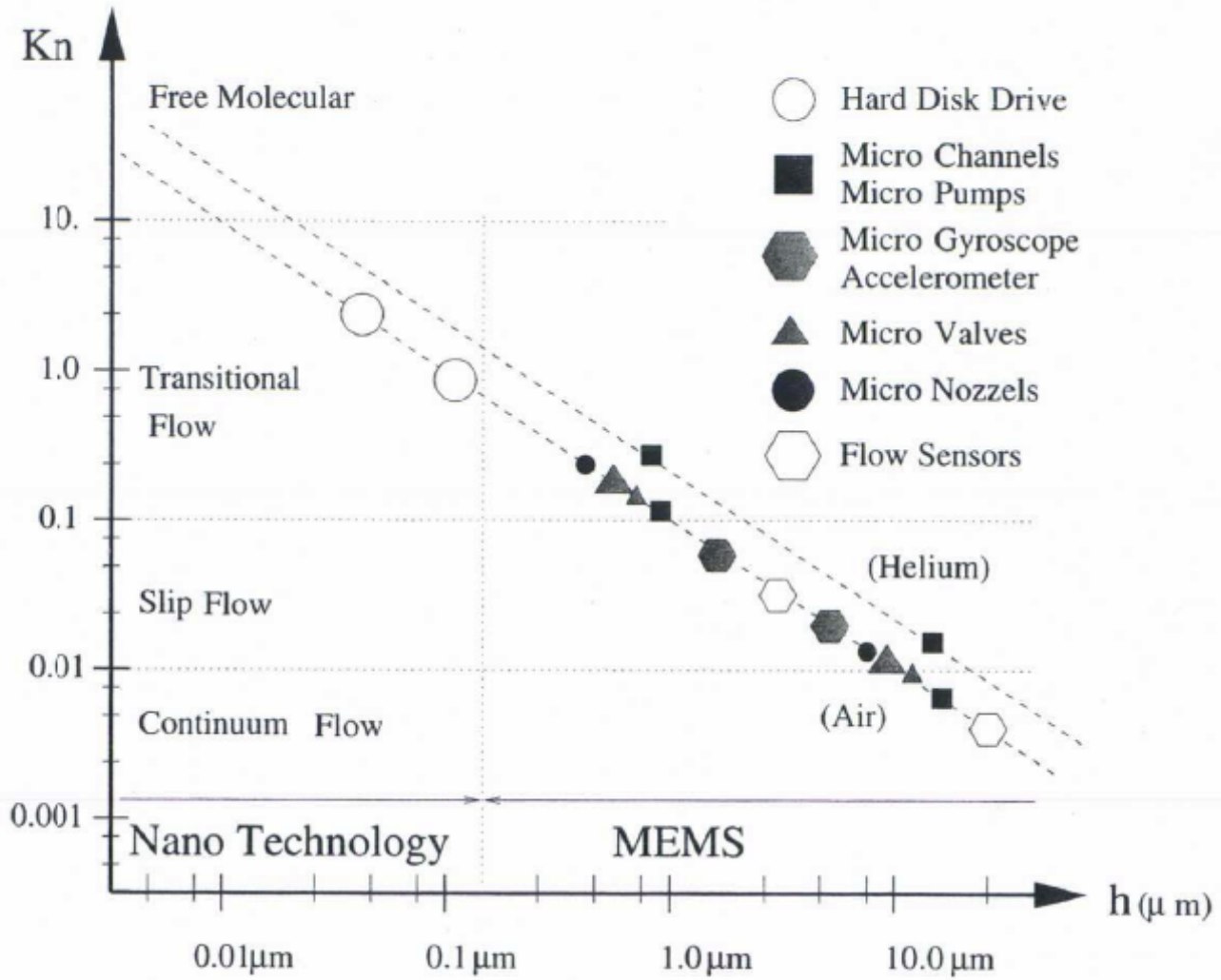

FIGURE 1.10. Typical MEMS and nano technology applications in standard atmospheric conditions span the entire Knudsen regime (Continuum, slip, transition and free-molecular flow). Here h denotes a characteristic length scale for the micro flow.

Karniadakis and Beskok.

The wall boundary condition

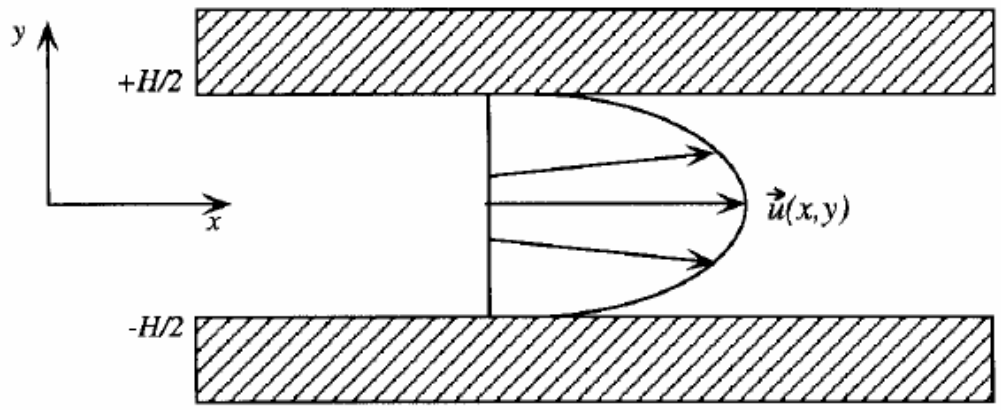

Fig. 1. Geometry for channel analysis, with a flow profile at a given position. As the flow proceeds downstream, this profile, along with the slip velocity, changes. The wall-normal components of the velocity vector are exaggerated.

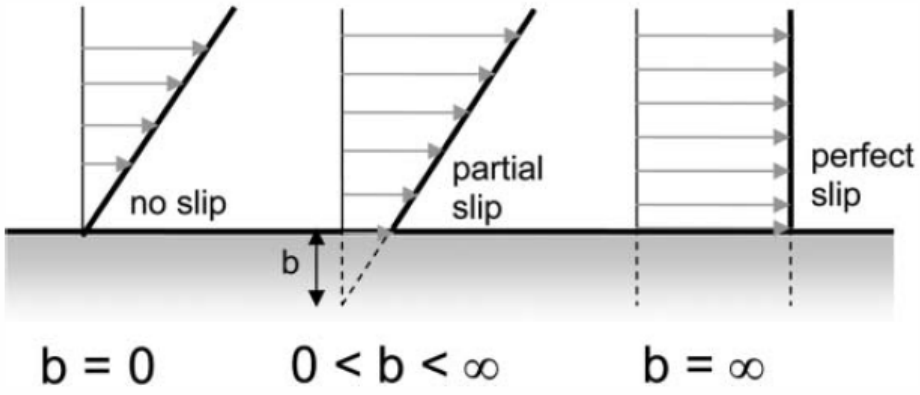

$$v\left(\frac{H}{2}\right) = b\left.\frac{dv}{dy}\right|_{\frac{H}{2}}$$

Fig. 1 Three cases of slip flow past a stationary surface. The slip length b is indicated. Drawing after ref. 1.

Eikjel, Lab on a Chip 7:299, 2007; Arkilic et al., J MEMS 6(2):167, 1997.

N/S

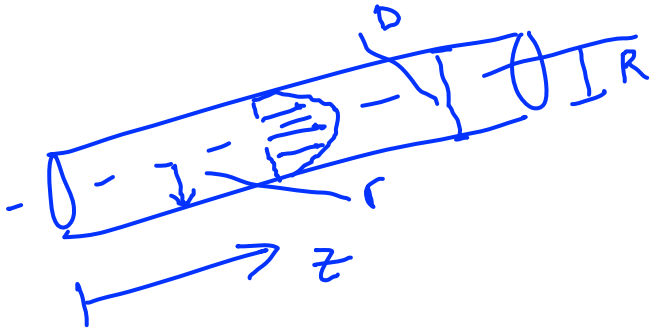

1 dimensional flow

$v(r)$, symmetric in θ

steady, fully developed flow.

$$\frac{dp}{dz} = \text{constant}$$

$$\frac{1}{\mu}\frac{dp}{dz} = \frac{1}{r}\frac{d}{dr}\left(r\frac{dv}{dr}\right)$$

$$\int\int \frac{r}{\mu}\frac{dp}{dz} = \int\int \left(\frac{d}{dr}\left(r\frac{dv}{dr}\right)\right)$$

$$\int \frac{r^2}{2\mu}\frac{dp}{dz} + C = \int r\frac{dv}{dr} \rightarrow \int\left(\frac{r}{2\mu}\frac{dp}{dz} + \frac{C}{r}\right) = \int \frac{dv}{dr}$$

$$\rightarrow \frac{r^2}{4\mu} + C\ln r + D = v(r), \quad D = -\frac{R^2}{4\mu}\frac{dp}{dz}$$

$$V_{n,i}(r) = -\frac{1}{4\mu}\frac{dp}{dz}\left(R^2 - r^2\right)$$

no slip, incompressible

flow rate, $Q = \int_A v(r)\,dA = 2\pi \int_0^R r\,v(r)\,dr$

$$Q = -\frac{dp}{dz}\left(\frac{\pi R^4}{8\mu}\right)$$

now, slip!

$$V(R) = -s\left.\frac{dv}{dr}\right|_R \qquad v(r) = \frac{1}{4\mu}\frac{dp}{dz}r^2 + D$$

slip coeff

$$\frac{dv}{dr} = \frac{1}{2\mu}\frac{dp}{dz}r \qquad (R)$$

$$v(R) = -\frac{sR}{2\mu}\frac{dp}{dz} = \frac{1}{4\mu}\frac{dp}{dz}R^2 + D$$

$$D = -\frac{1}{\mu}\left(\frac{dp}{dz}\right)\left(\frac{R^2}{4} + \frac{SR}{2}\right)$$

$$V_{s,i}(r) = -\frac{1}{4\mu}\left(\frac{dp}{dz}\right)\left(R^2 - r^2 + 2SR\right)$$

↑ slip

$$Q = \int_A v(r)\,dA \quad \Rightarrow \quad Q_{s,i} = -\pi\frac{dp}{dz}\left(\frac{R^4}{8\mu} + \frac{SR^3}{2\mu}\right)$$

$$\frac{dp}{dz_{s,i}} = \frac{-Q}{\frac{\pi}{\mu}\left(\frac{R^4}{8} + \frac{SR^3}{2}\right)}$$

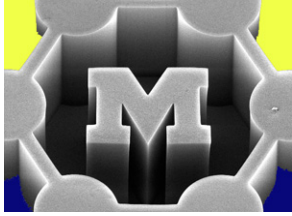

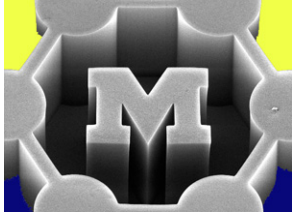

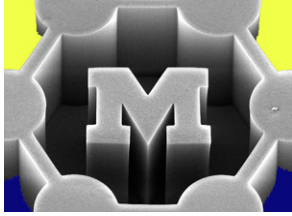

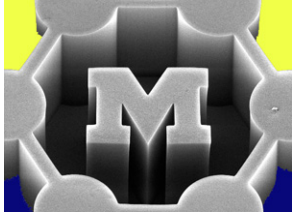

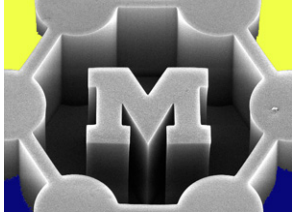

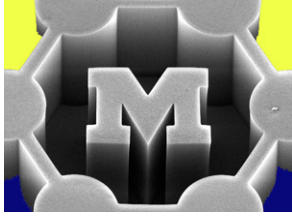

Slip vs. no slip: CH_4, 900 °C, D = 5 μm

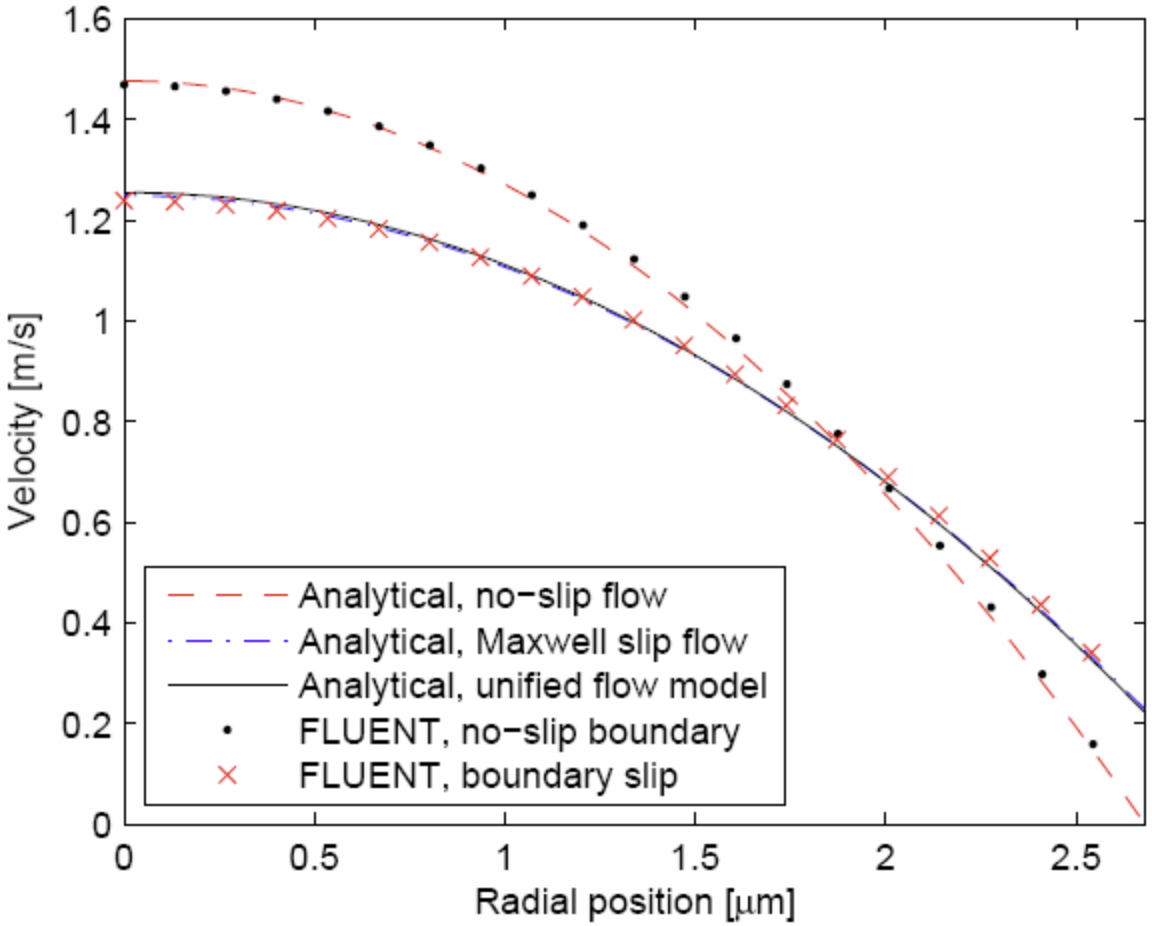

Figure 5-4. Velocity profiles predicted by incompressible no-slip, Maxwell slip, and unified flow models, for 0.001 sccm CH_4 flow at 900 °C through a 5 μm diameter pipe.

Slip vs. no slip: CH_4, 900 °C, D = 50 μm

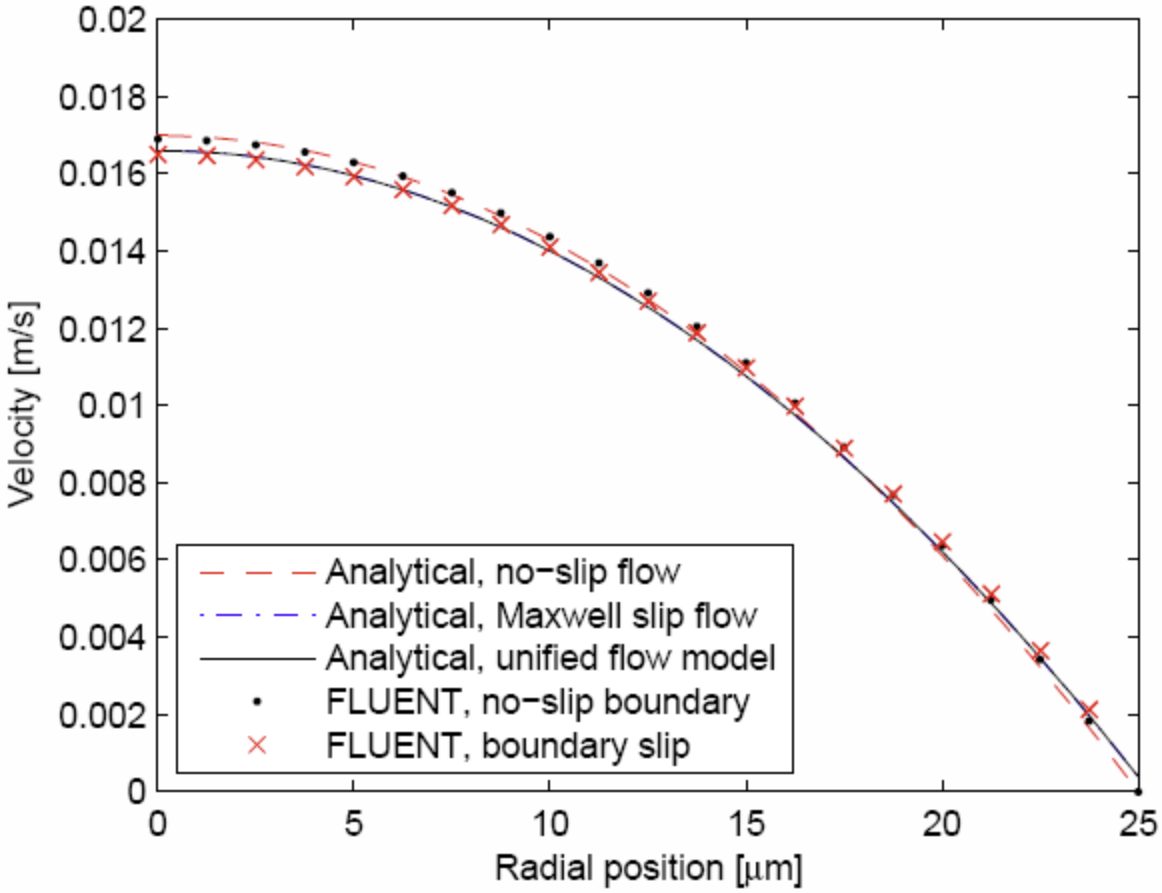

Figure 5-6. Velocity profiles predicted by incompressible no-slip, Maxwell slip, and unified flow models, for 0.001 sccm CH_4 flow at 900 °C through a 50 μm diameter pipe.

Slip vs. no slip: pressure gradient

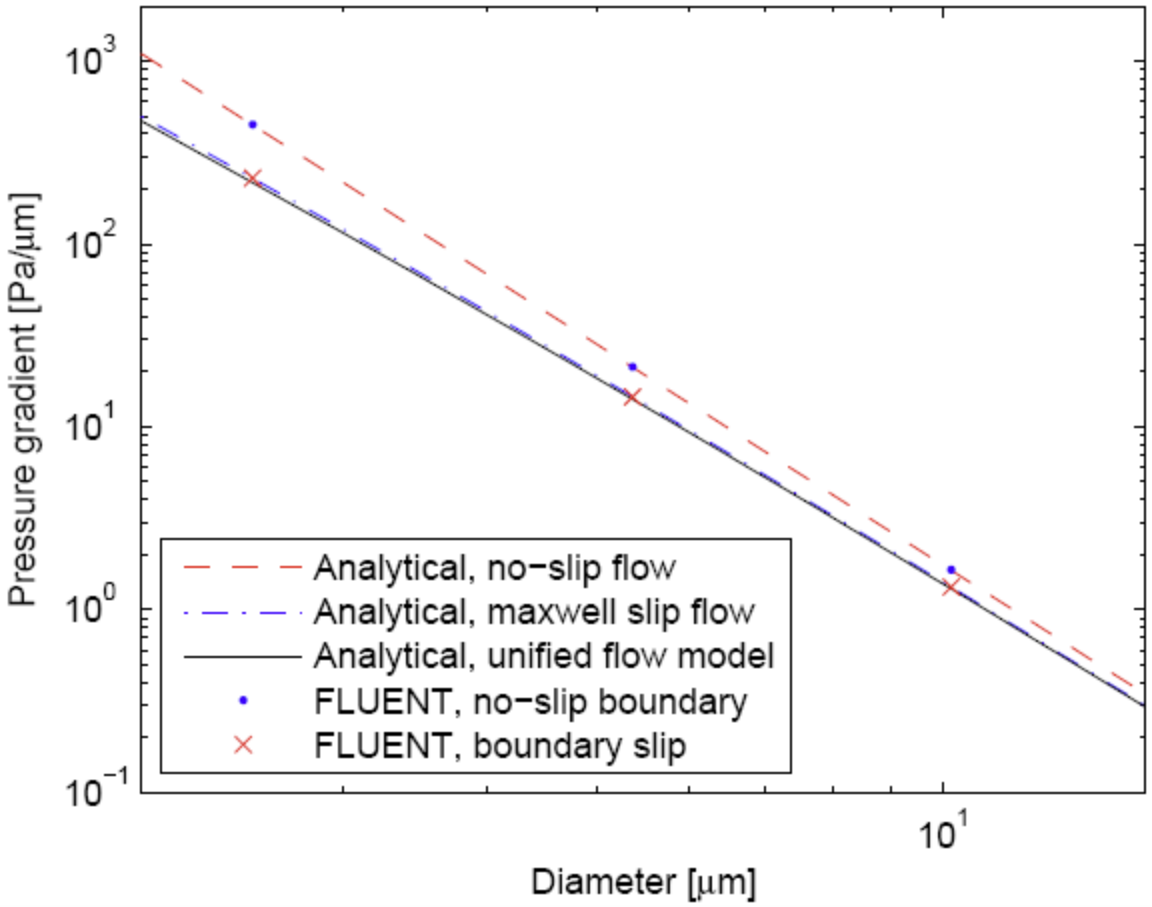

Figure 5-7. Pressure gradients predicted by incompressible no-slip, Maxwell slip, and unified flow models, for 0.001 sccm CH_4 flow at 900 °C through a microscale pipe.

Slip coefficient for a gas

$$S = \frac{\mu}{\varepsilon} = \frac{\text{internal friction}}{\text{wall friction}}$$

$$\frac{\mu}{\varepsilon} = \frac{\mu}{\rho}\sqrt{\frac{\pi}{2R_u T_w}}\left(\frac{2-\sigma_v}{\sigma_v}\right)$$

R_u: universal gas constant

T_w: temperature

σ_v: tangential momentum accommodation coefficient

$$\sigma_v = \frac{\tau_i - \tau_r}{\tau_i}$$

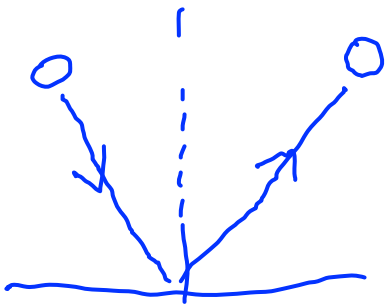

specular, $\sigma_v = 0$

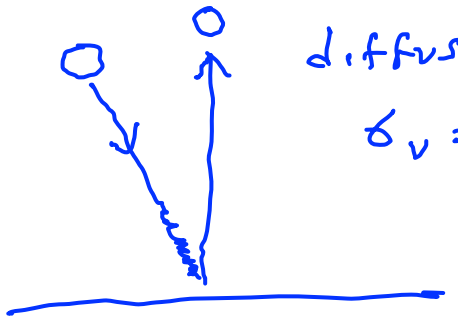

Most gases, $\delta_r = 0.75 - 0.85$

(Acrylic)

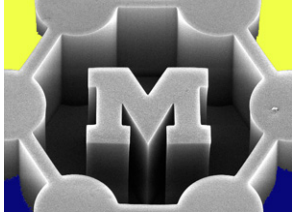

Effect of compressibility

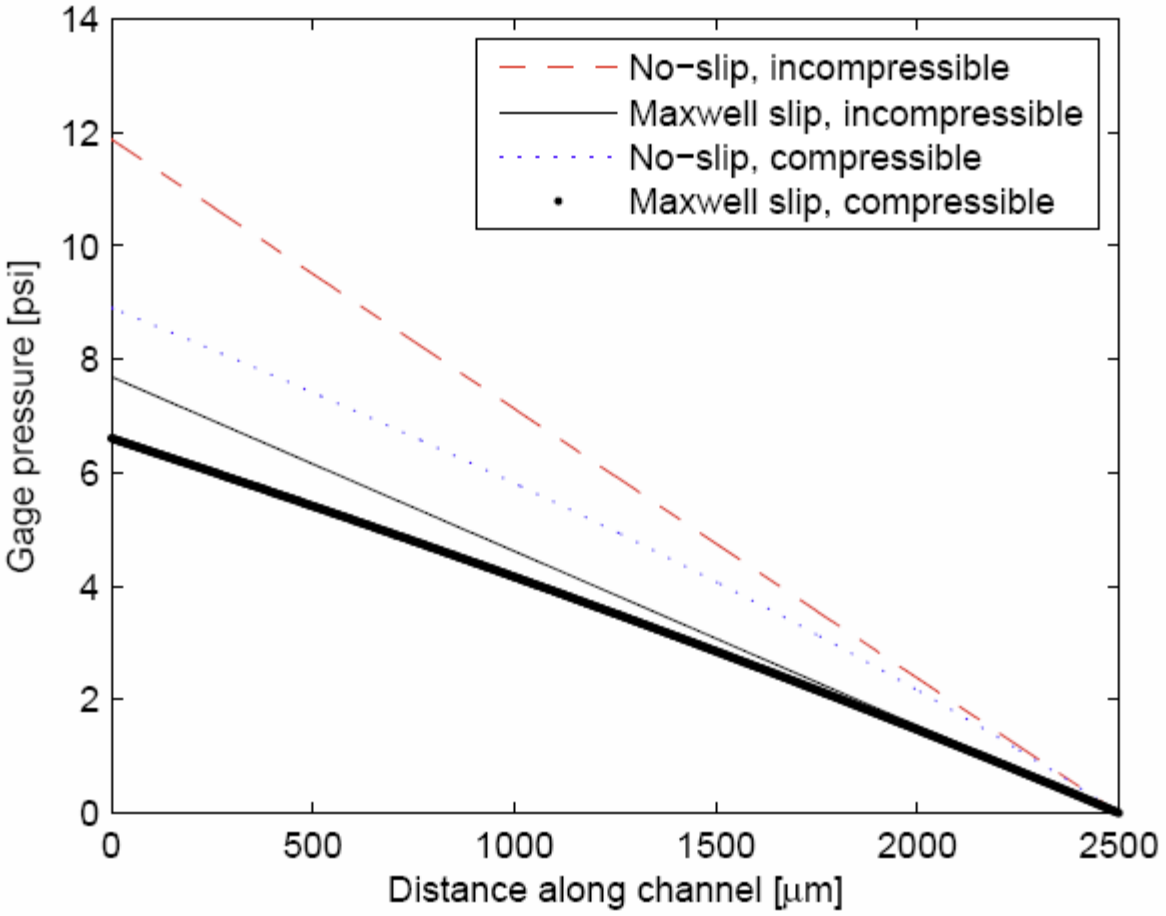

Figure 5-12. Pressure distribution (CH_4, 900 °C) along a 5 μm diameter circular pipe, according to compressible and incompressible flow models, calculated for $\dot{m} = 3.27 \times 10^{-12}$ kg/s.

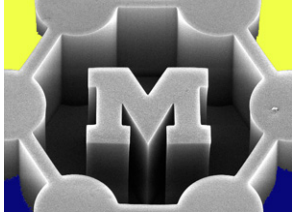

What's the molecular origin of slip?

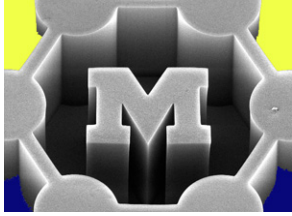

- Fluid-fluid interactions are stronger than fluid-wall interactions (e.g., hydrophobicity).
- Surface roughness traps gas molecules dissolved in the liquid, creating a lubrication layer at the wall. Here, what happens at high Re?
- Molecules "hop" between minimum-energy sites in the wall lattice; therefore slip is a rate process and slip length depends on temperature.

Squires and Quate, Rev Mod Phys 77:977, 2005.
Lichter et al., Phys Rev Lett 98:226001, 2007.

Ordered fluid layers at the wall

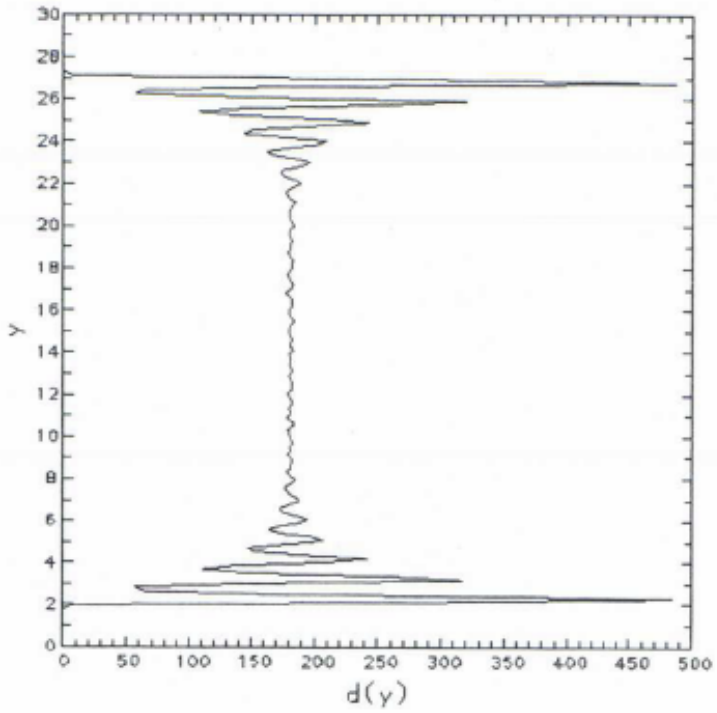

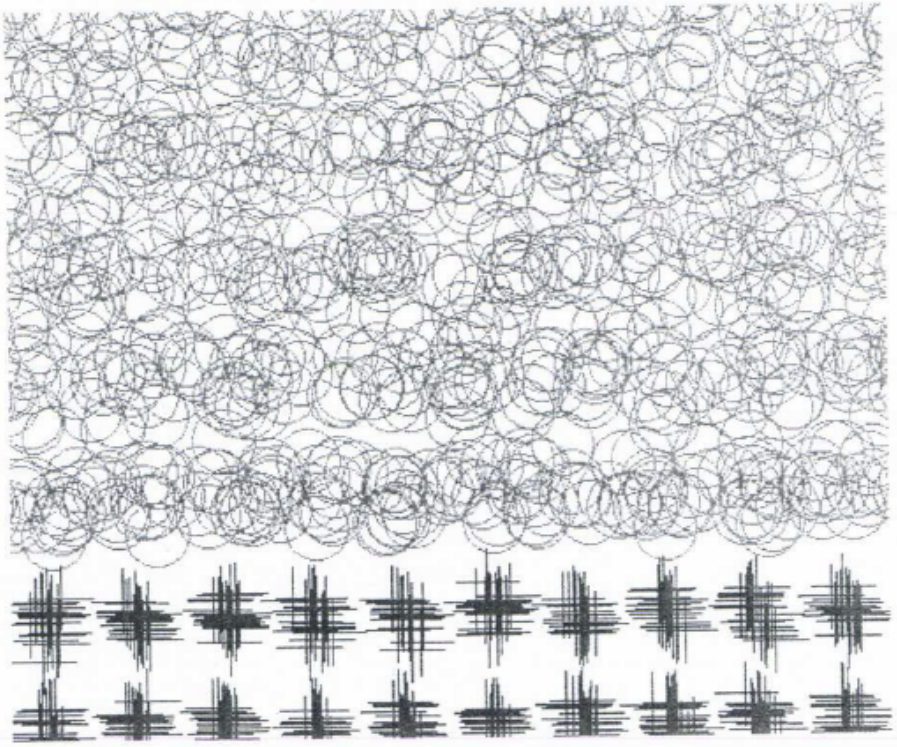

FIGURE 1.7. Snapshot of the Lennard-Jones fluid near a wall. The wall atoms are denoted by crosses and fluid atoms by circles. This layered structure of the fluid molecules in close proximity with the wall is responsible for the density fluctuations shown in the previous figure. (Courtesy of J. Koplik and J. Banavar)

Karniadakis and Beskok.

Measuring gas flows in microchannels

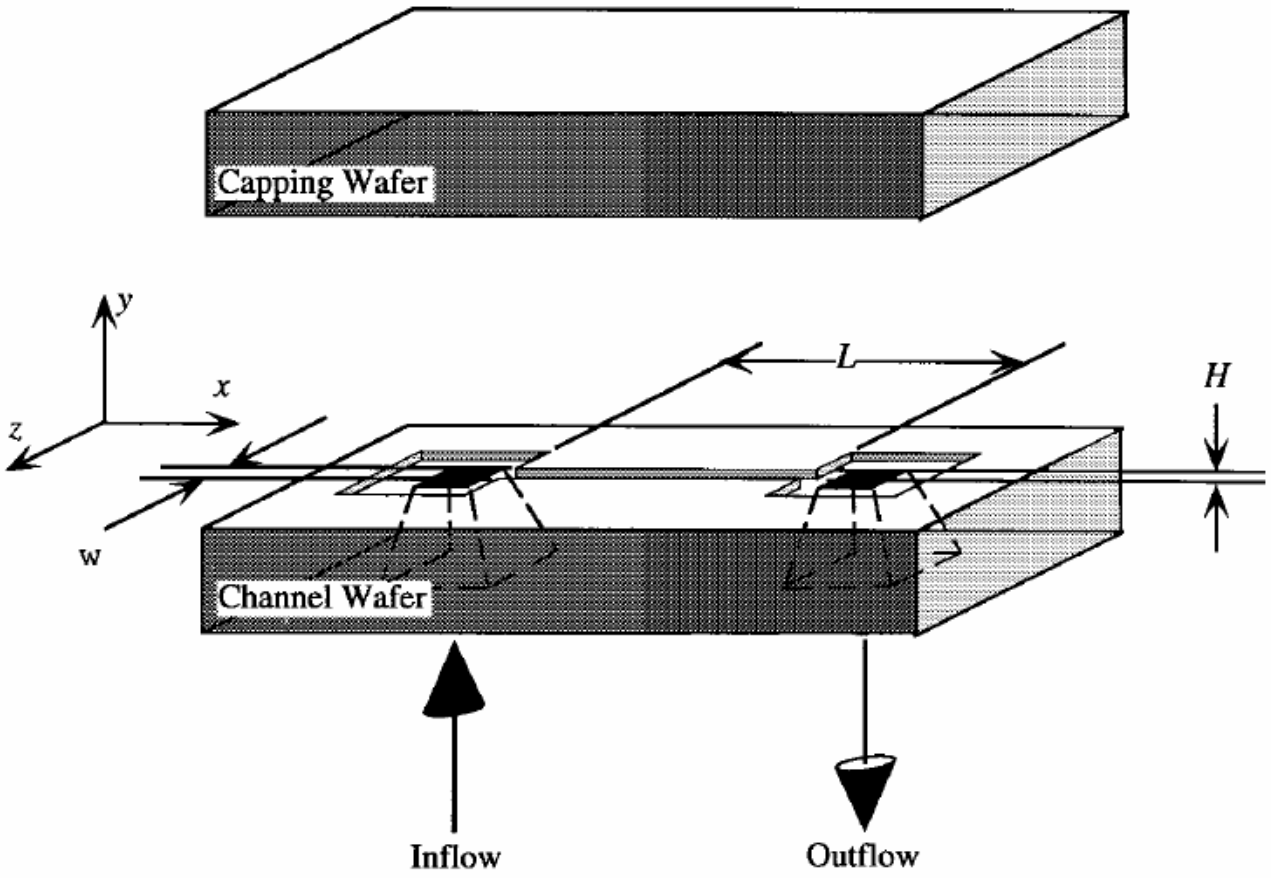

ARACTERIZATION

Parameter	Nominal Value (μm)	Variation (μm)
length (L)	7500	± 10
width (w)	52.25	± 0.25
height (H)	1.33	± 0.01
surface roughness	$\leq 0.65 \times 10^{-3}$	NA

Arkilic et al., J MEMS 6(2):167, 1997.

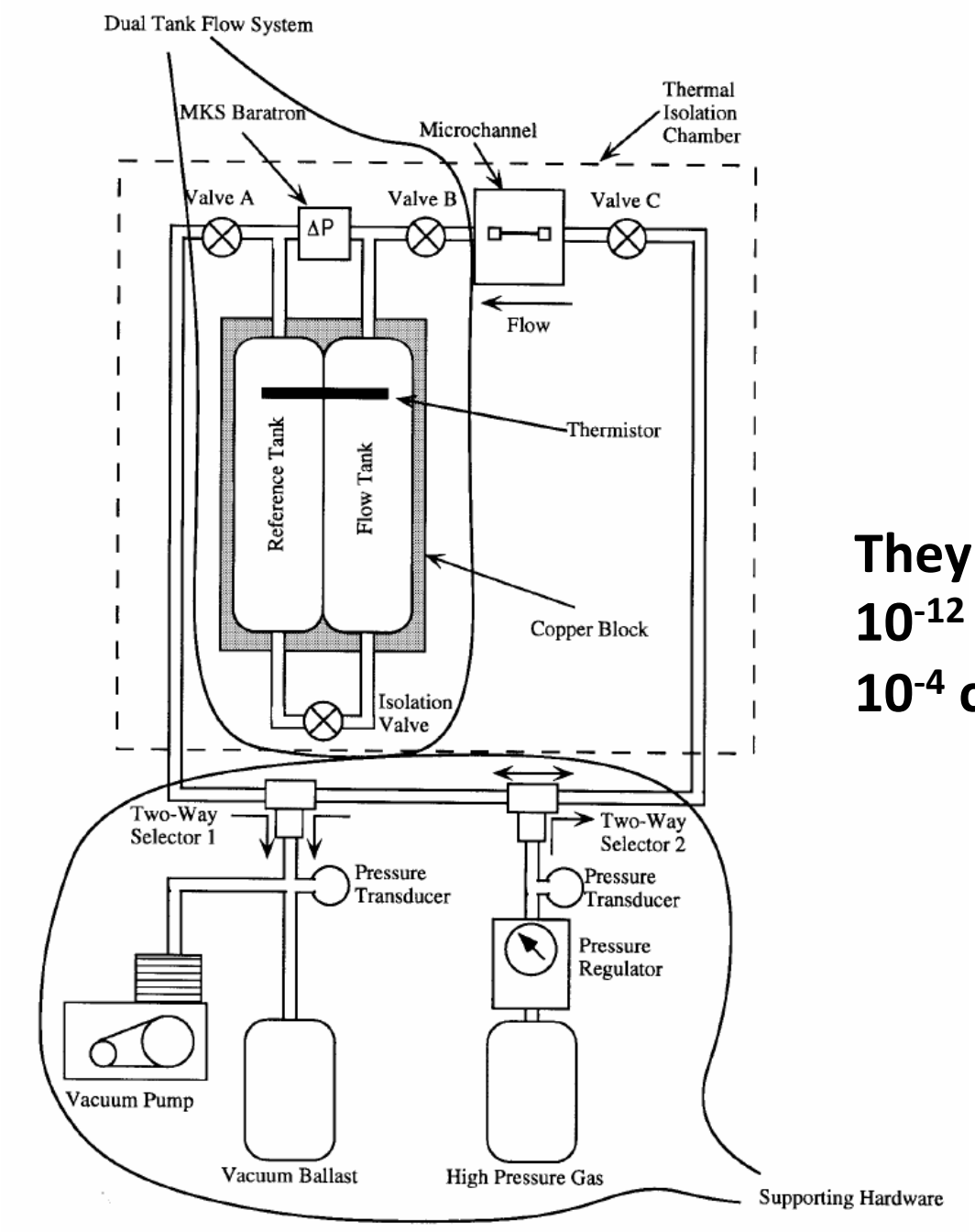

They measured
10^{-12} kg/s
10^{-4} cm^3/s

Arkilic et al., J MEMS 6(2):167, 1997.

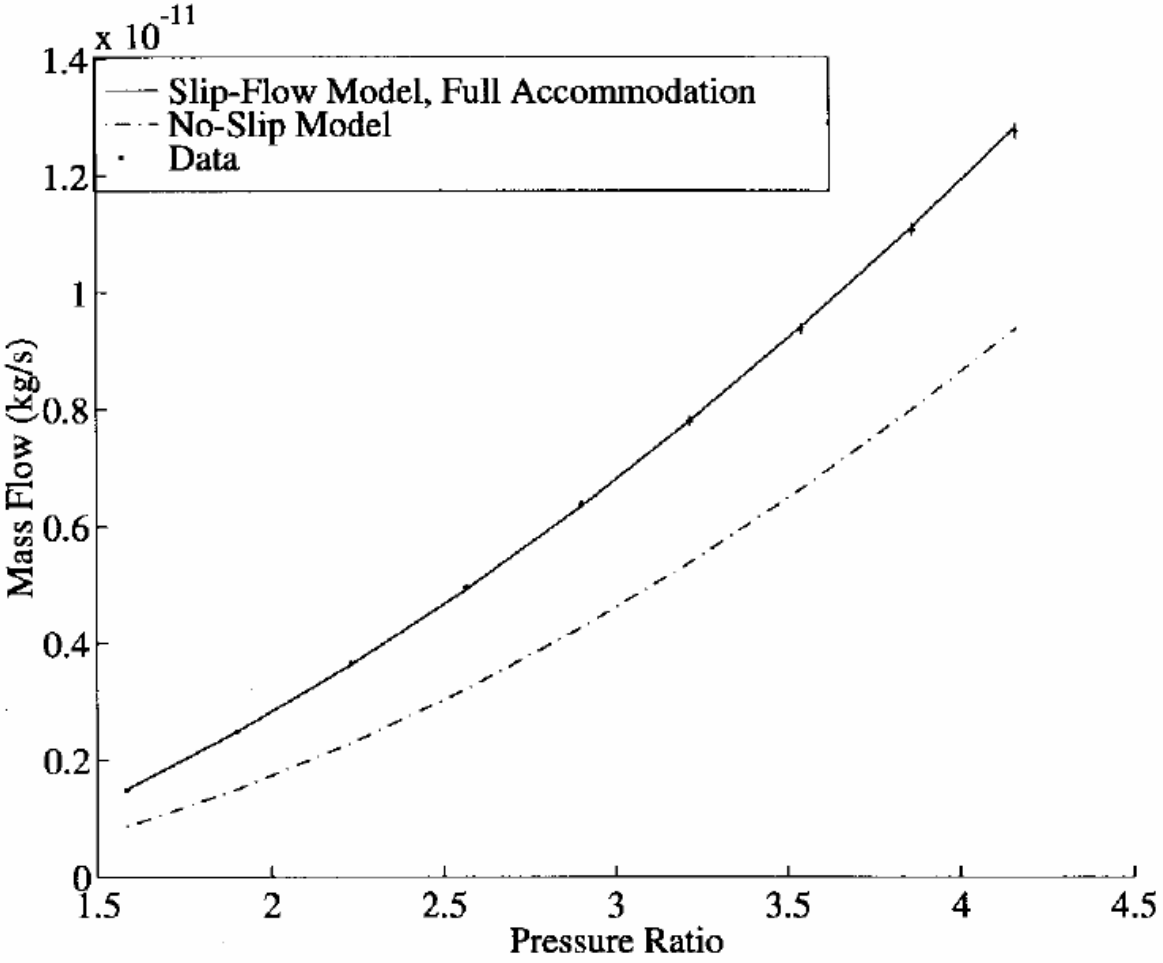

Fig. 10. Helium mass flow for 1.33-μm channel (95% confidence intervals indicated). The solid curve is the solution to (21), assuming full tangential momentum accommodation, and the dashed curve is the solution to (21) setting $K = 0$ (no-slip solution).

Arkilic et al., J MEMS 6(2):167, 1997.

Flow *through* CNTs

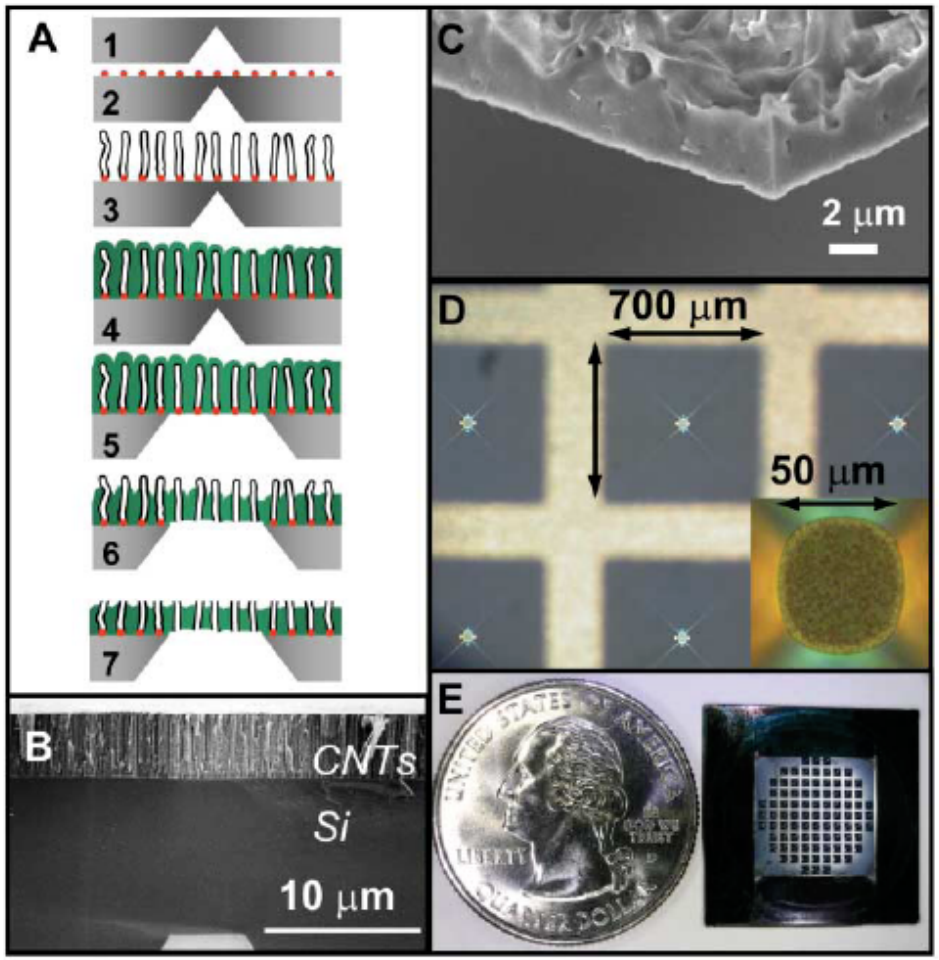

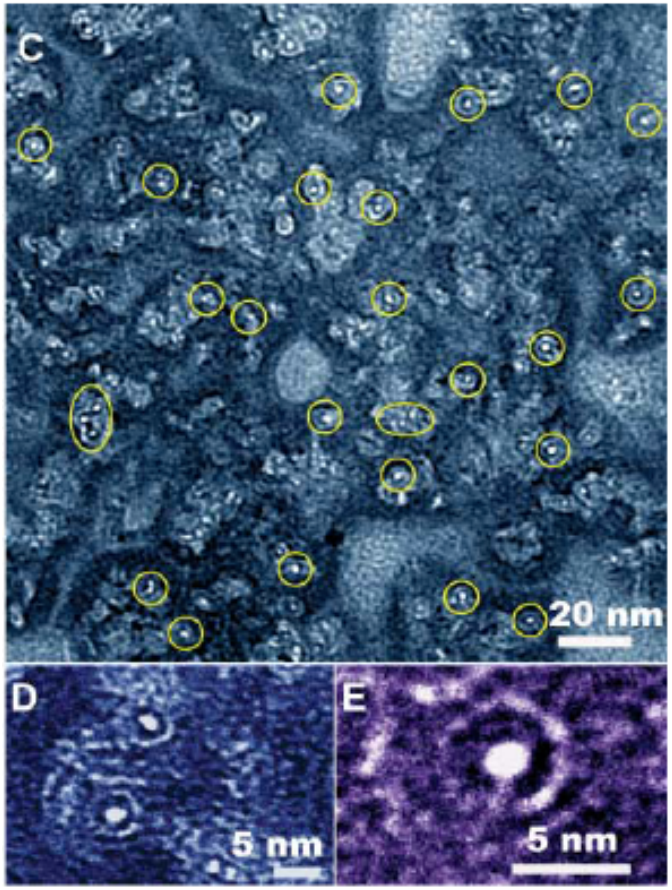

Fig. 1. (**A**) Schematic of the fabrication process. Step 1: microscale pit formation (by KOH etching). Step 2: catalyst deposition/annealing. Step 3: nanotube growth. Step 4: gap filling with low-pressure chemical vapor–deposited Si_3N_4. Step 5: membrane area definition (by XeF_2 isotropic Si etching). Step 6: silicon nitride etch to expose nanotubes and remove catalyst nanoparticles (by Ar ion milling); the membrane is still impermeable at this step. Step 7: nanotube uncapping (reactive ion etching); the membrane begins to exhibit gas permeability at this step. (**B**) SEM cross section of the as-grown DWNTs (CNTs). (**C**) SEM cross section of the membrane, illustrating the excellent gap filling by silicon nitride. (**D**) Photograph of the open membrane areas; inset shows a close-up of one membrane. (**E**) Photograph of the membrane chip that contains 89 open windows; each window is 50 μm in diameter.

Holt et al., Science 312:1034-1037, 2006.

Flow *through* CNTs

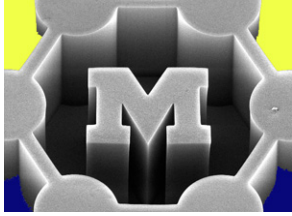

Fig. 4. Air (red) and water (blue) permeability as measured for three DWNT membranes (DW#1, 2, and 3) and a polycarbonate membrane (PC). Despite considerably smaller pore sizes, the permeabilities for all DWNT membranes greatly exceed those of the polycarbonate membrane.

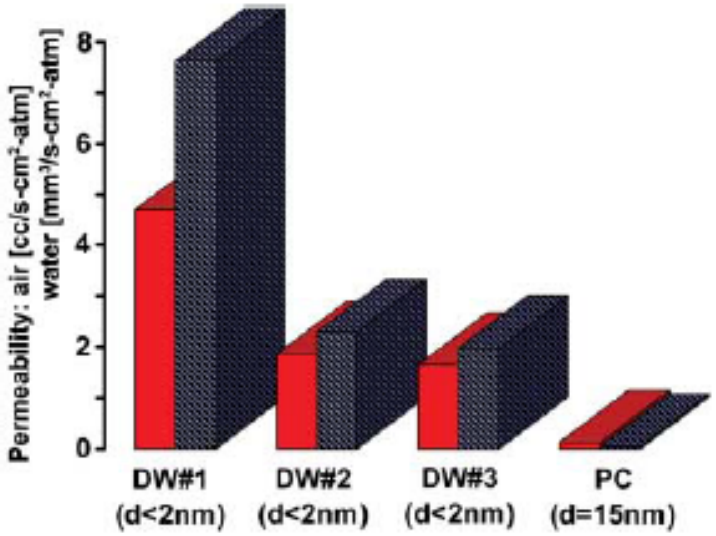

Membrane	Pore diameter (nm)	Pore density (cm^{-2})	Thickness (μm)	Enhancement over Knudsen model* (minimum)	Enhancement over no-slip, hydrodynamic flow† (minimum)	Calculated minimum slip length‡ (nm)
DWNT 1	1.3 to 2.0	$\leq 0.25 \times 10^{12}$	2.0	40 to 120	1500 to 8400	380 to 1400
DWNT 2	1.3 to 2.0	$\leq 0.25 \times 10^{12}$	3.0	20 to 80	680 to 3800	170 to 600
DWNT 3	1.3 to 2.0	$\leq 0.25 \times 10^{12}$	2.8	16 to 60	560 to 3100	140 to 500
Polycarbonate	15	6×10^{8}	6.0	2.1	3.7	5.1

*From (*18*). †From (*26*). ‡From (*29*).

Holt et al., Science 312:1034-1037, 2006.

Extreme slip flow through CNTs

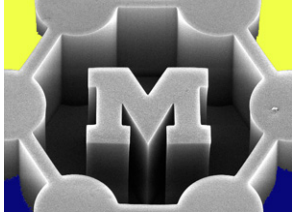

Table 1 | Pressure-driven flow through aligned MWCNT membrane

Liquid	Initial permeability*	Observed flow velocity†	Expected flow velocity†	Slip length (mm)
Water	0.58	25	0.00057	54
	1.01	43.9	0.00057	68
	0.72	9.5	0.00015	39
Ethanol	0.35	4.5	0.00014	28
iso-Propanol	0.088	1.12	0.00077	13
Hexane	0.44	5.6	0.00052	9.5
Decane	0.053	0.67	0.00017	3.4

MWCNT, multiwalled carbon nanotube. For details of methods, see supplementary information. *Units, cm^3 per cm^2 min bar. †Flow velocities in cm s^{-1} at 1 bar. Expected flow velocity is that predicted from conventional flow.

Majumder et al., Nature 438:44, 2005.

Importance of gas damping in MEMS: DMD micromirrors

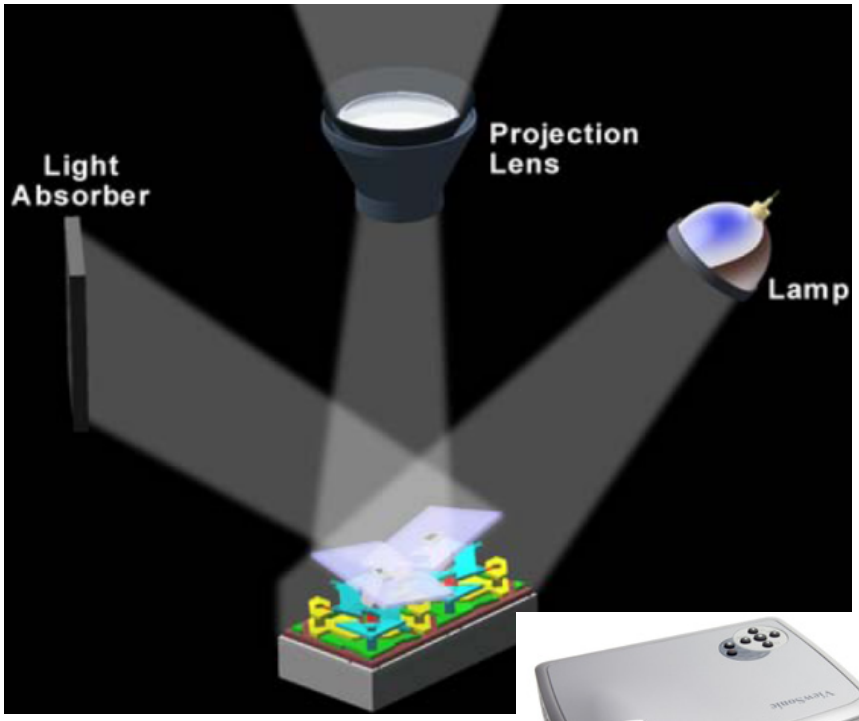

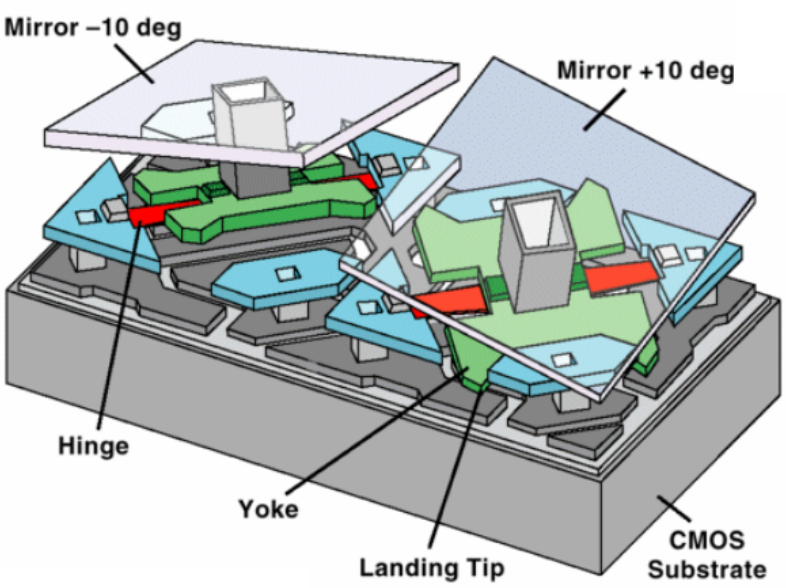

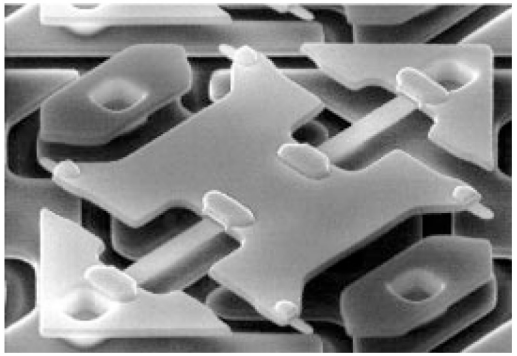

Mirror dynamics at various ambient pressures

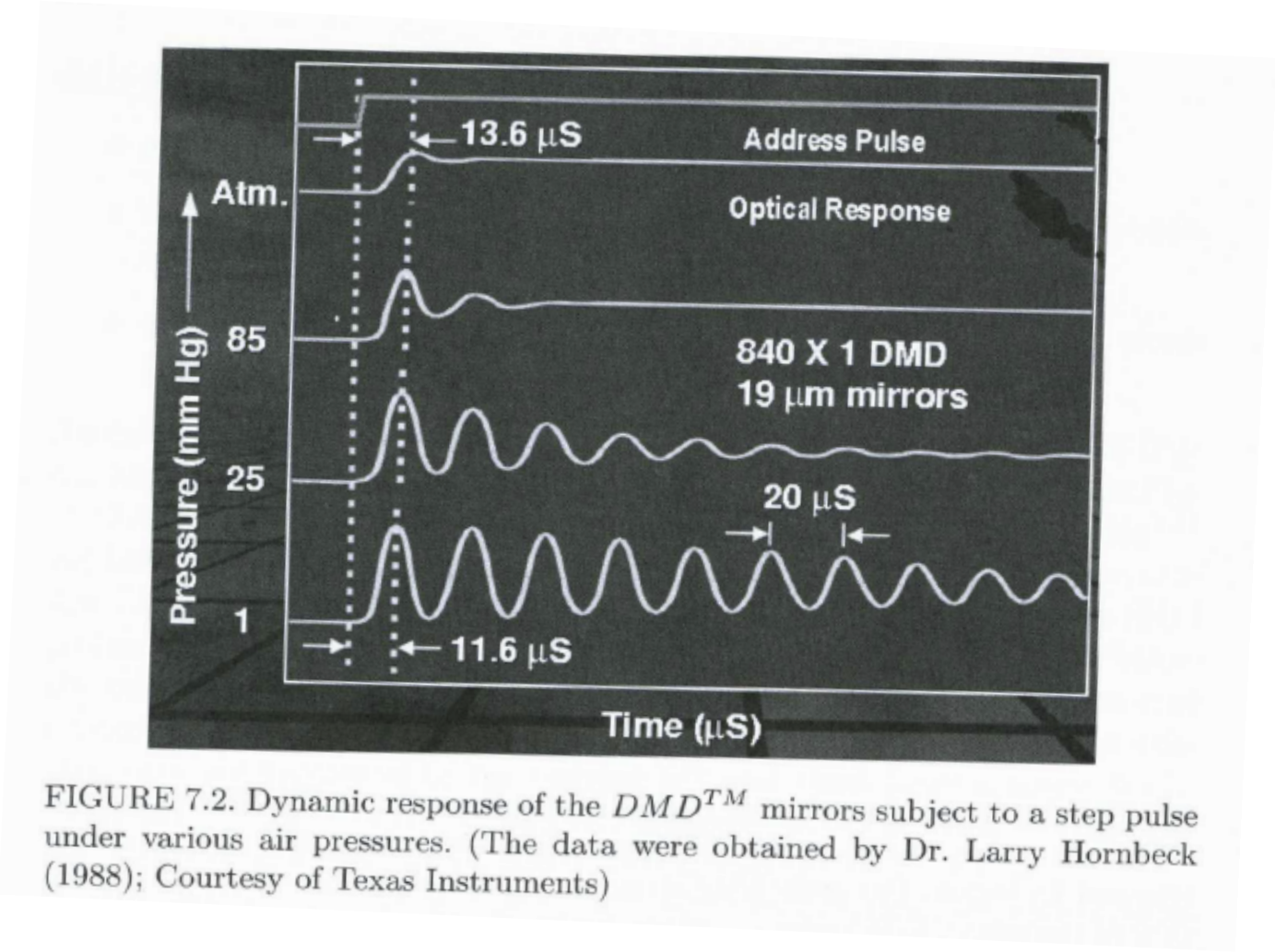

FIGURE 7.2. Dynamic response of the DMD^{TM} mirrors subject to a step pulse under various air pressures. (The data were obtained by Dr. Larry Hornbeck (1988); Courtesy of Texas Instruments)

Karniadakis and Beskok.